Localization-delocalization transition of photons in one-dimensional random *n*-mer dielectric systems

Z. Zhao,[1] F. Gao,[1] R. W. Peng,[1,*] L. S. Cao,[1] D. Li,[1] Z. Wang,[1] X. P. Hao,[1] Mu Wang,[1] and C. Ferrari[2]
[1]*National Laboratory of Solid State Microstructures and Department of Physics, Nanjing University, Nanjing 210093, China*
[2]*IMEM-CNR Institute, Parco Area delle Scienze 37/A, Parma I-43010, Italy*
(Received 2 October 2006; revised manuscript received 30 January 2007; published 25 April 2007)

In this work, we have both theoretically and experimentally investigated the photonic transmission in a one-dimensional random *n*-mer (RN) dielectric system. Due to the positional correlation in the RN structure, the localization-delocalization transitions of photons happen at expected frequencies of photons. Multiple resonant transmissions are found in the photonic band gap. At each resonant mode, zero-Lyapunov exponent and undecayed field distribution of electromagnetic waves have been found through the whole system. Furthermore, the channel is opened for photonic transport at the resonant frequency, and the density of states of photons increases step by step as frequency increases. The theoretical results are experimentally demonstrated in RN dielectric multilayer films of SiO_2/TiO_2 for visible and near infrared light.

DOI: 10.1103/PhysRevB.75.165117 PACS number(s): 42.25.Dd, 42.70.Qs, 61.43.−j

I. INTRODUCTION

Back in 1958, Anderson studied the localization of electrons in one-dimensional (1D) disordered systems.[1] Later, the concept of localization was recognized as applicable to any wave, such as acoustical waves[2] and optical wave.[3,4] It has also been pointed out that the localization of waves appears not only in disordered system, but also in deterministic aperiodic systems. Obviously, the photonic localization in a dielectric microstructure can be considered as an analogy to the electronic localization in crystals.[4] Up to now, the photonic localization has been demonstrated in periodic, quasiperiodic, and other deterministic aperiodic systems[5–9] which achieve a photonic band gap and present potential applications in optoelectronics.[10,11] On the other hand, a localization-delocalization transition of electron was predicted by Dunlap *et al.* initially in a 1D random-dimer model.[12] It can be extended to random-trimer, random dimer-trimer, and even random *n*-mer model.[13] Very recently, the transition has been experimentally demonstrated in random-dimer GaAs-AlGaAs superlattices.[14] Physically, the extended electronic states in this system are due to the symmetry of its internal structure. Motivated by the localization-delocalization transition of electrons, we are interested to know whether an analog exists in the case of photons in dielectric microstructures.

In this work, we investigate the localization-delocalization transition of photons in 1D random *n*-mer (RN) dielectric structures both in theory and in experiment. This paper is organized as follows. In Sec. II, we present a theoretical analysis based on Maxwell equations. In Sec. III, optical transmissions and photonic band structures are given as an example in random-dimer (RD) system. The localization-delocalization transition is discussed based on undecayed field distribution at the resonant mode. In Sec. IV, RD model is generalized to random-trimer, random-tetramer, and random *n*-mer systems. Optical transmission and the density of states of photons are studied in these systems. The delocalization of photons is discussed based on zero-Lyapunov exponent at the resonant modes. In Sec. V, we show the experiment results in RN dielectric multilayer films of SiO_2/TiO_2, which are in good agreement with the theoretical predictions. Finally, a summary is given in Sec. VI.

II. THEORETICAL MODEL

Consider the optical propagation through a dielectric multilayer $S_0=\{A_1A_2\cdots A_i\cdots A_{m-1}A_m\}$, where there are m dielectric layers A_i $(i=1,2,\ldots,m)$ with their refractive indices $\{n_i\}$ and thicknesses $\{d_i\}$, respectively. We use the transfer matrix method and follow the description of the electric field in the report of Kohmoto and Banavar.[6] In the case of normal incidence and polarization parallel to the multilayer surfaces, the transmission through the interface $A_j \leftarrow A_i$ is given by the transfer matrix

$$T_{i,j}=\begin{pmatrix}1 & 0\\ 0 & n_i/n_j\end{pmatrix}. \tag{1}$$

The light propagation within the layer A_i is described by matrix T_i,

$$T_i=\begin{pmatrix}\cos\delta_i & -\sin\delta_i\\ \sin\delta_i & \cos\delta_i\end{pmatrix}, \tag{2}$$

where the phase shift $\delta_i=kn_id_i$ and k is the vacuum wave vector. Therefore, the whole multilayer is represented by a product matrix M relating the incident and reflection waves to the transmission wave. The total transmission matrix M has the form

$$M(N,\delta_i)=\begin{pmatrix}m_{11} & m_{12}\\ m_{21} & m_{22}\end{pmatrix}, \tag{3}$$

where N is the number of layers in the system. Let us define the trace of global transfer matrix M as $\mathrm{Tr}\,M$. The allowed region of photons in the band structure satisfies

$$\left|\frac{1}{2}\mathrm{Tr}\,M(N,\delta_i)\right| \le 1. \tag{4}$$

Using the unitary condition $\det|M(N,\delta_i)|=1$, the transmission coefficient of the multilayer film can be written as

$$T(N,\delta_i) = \frac{4}{\sum_{i,j=1}^{2} m_{ij}^2 + 2}. \tag{5}$$

Now we consider the RN dielectric multilayer, where the dielectric layer A and the dielectric layers $B\cdots B$ (the number of B is n) are randomly assigned in the multilayer $S(n)$ as follows:

$$S(n) = \underbrace{A\cdots A}_{X_1}\underbrace{BB\cdots B}_{Y_1}\underbrace{BA\cdots A}_{X_2}\underbrace{BB\cdots B}_{Y_2}\cdots\underbrace{A\cdots A}_{X_i}\underbrace{BB\cdots B}_{Y_i}\cdots\underbrace{A\cdots A}_{X_{m-1}}\underbrace{BB\cdots B}_{Y_{m-1}}\underbrace{BA\cdots A}_{X_m}, \tag{6}$$

where X_i (Y_i) is the number of layer A (B) in the ith cluster of A (B). Obviously, $Y_i=2Z_i$ in the random-dimer model, $Y_i=3Z_i$ in the random-trimer model, and, in general, $Y_i=nZ_i$ in the RN model, respectively. Here Z_i is an integer. We consider the simplest setting; i.e., the phase shift of a wave through each layer is identical: $\delta_i=\delta_A=\delta_B\equiv\delta$. This condition can be easily satisfied in experiments by tuning the thickness of each dielectric layer. Therefore, if the electromagnetic wave goes through the ith cluster of A, the transfer matrix comes to M as

$$M_A(i) = (T_A)^{X_i} = \begin{pmatrix} \cos(X_i\delta) & -\sin(X_i\delta) \\ \sin(X_i\delta) & \cos(X_i\delta) \end{pmatrix}. \tag{7}$$

While if the wave goes through the ith cluster of B sandwiched by the layers A in the RN system, the transfer matrix becomes

$$M_B(n,i) = T_{B,A}(T_B)^{Y_i}T_{A,B} = \begin{pmatrix} \cos(Y_i\delta) & -(n_A/n_B)\sin(Y_i\delta) \\ (n_B/n_A)\sin(Y_i\delta) & \cos(Y_i\delta) \end{pmatrix}, \tag{8}$$

where $Y_i=nZ_i$. Therefore, the whole matrix of the RN dielectric multilayer can be written as

$$M(n) = M_A(1)M_B(n,1)M_A(2)M_B(n,2)\cdots M_A(i) \times M_B(n,i)\cdots M_B(n,m)M_A(m). \tag{9}$$

According to the matrix theory,[15,16] it can be proved that when the phase shift satisfies

$$\delta = \frac{l}{n}\pi \quad (l=1,2,\ldots,n-1), \tag{10}$$

the matrix $M_B(n,i)$ becomes

$$M_B(n,i) = (-1)^{Z_i}I, \tag{11}$$

where I is a unitary matrix. Therefore, the global transfer matrix through the RN system becomes

$$M(N,\delta) = (M_A)^{\Sigma_i X_i} \quad \text{or} \quad -(M_A)^{\Sigma_i X_i}, \tag{12}$$

and the transmission coefficient of the multilayer film can be perfect, i.e., $T(N,\delta)=1$. Physically, once the frequency of photon satisfies Eq. (9), the photon can propagate through the whole RN system. Meanwhile, the behavior of a photon in the RN system is similar to that in a homogeneous film of the dielectric material A. From this point of view, localization-delocalization transition of photons, indeed, takes place at the resonant frequencies of photons given by Eq. (10).

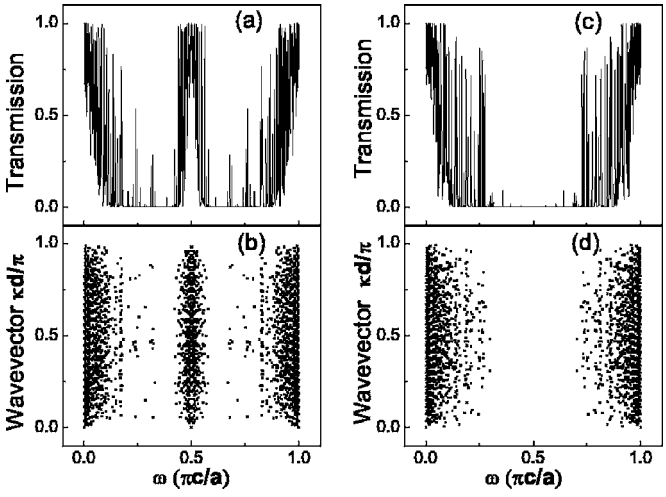

FIG. 1. (a) The photonic transmission spectrum and (b) the dispersion relation in RD multilayer of SiO_2/TiO_2. (c) The photonic transmission spectrum and (d) the dispersion relation in a random multilayer of SiO_2/TiO_2. The dielectric materials A and B are SiO_2 and TiO_2, respectively. The layer thicknesses d_A and d_B in these two multilayer films are chosen to satisfy $n_Ad_A=n_Bd_B\equiv a$, and the total thickness of the multilayer is d. The total number of layers in each film is $N=365$.

III. RANDOM-DIMER CASE

As an example, the RD dielectric multilayer has been studied. The RD structure can be described by Eq. (6) in the case of $n=2$. According to Eqs. (1)–(5), we can calculate numerically photonic band structures and transmission coefficients of electromagnetic waves in the RD dielectric multilayers. In the calculation, silicon dioxide (SiO_2) and titanium dioxide (TiO_2) were chosen as dielectric materials A and B, respectively. The refractive indices are set as $n_A=1.46$ and $n_B=2.3$. The layer thicknesses d_A and d_B are designed to

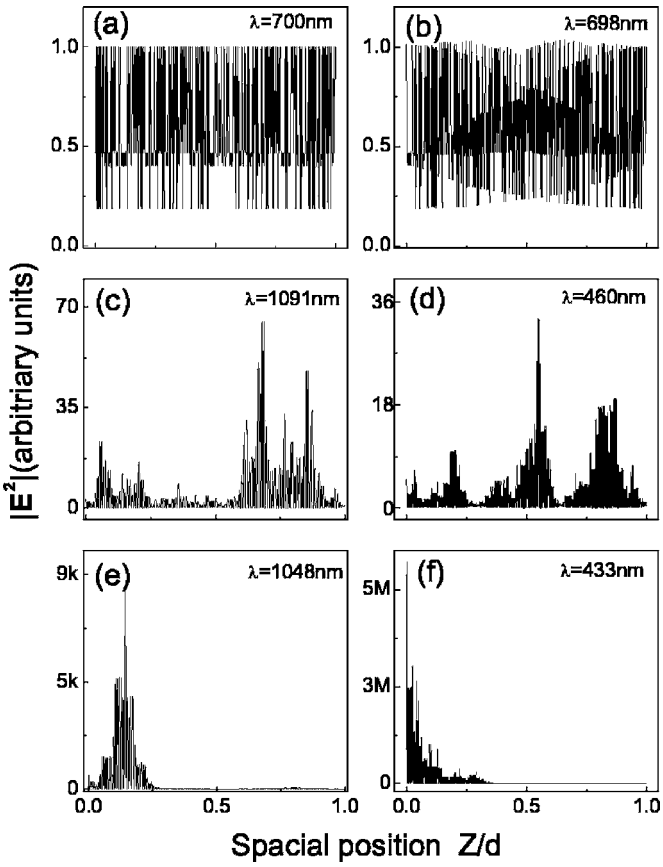

FIG. 2. The electric field distributions along the layer growth in the RD multilayer of SiO_2/TiO_2. (a) and (b), the extended distributions around the resonant frequency $\omega_{RD}=\pi c/2a$, i.e., $\lambda_{RD}=700$ nm; (c) and (d), the amplitude distributions between the extended and localized states away from the resonant mode λ_{RD}; and (e) and (f), the localized distributions away from the resonant mode λ_{RD}. Here, the layer thicknesses d_A and d_B are chosen to satisfy $a=n_Ad_A=n_Bd_B=175$ nm. The total number of layers is $N=365$, and d is the total thickness of the film.

satisfy $n_Ad_A=n_Bd_B\equiv a$. Figures 1(a) and 1(b) show, respectively, the photonic transmission spectrum and the dispersion relationship in the RD system. Zero transmission coefficient [shown in Fig. 1(a)] corresponds to the forbidden zone, i.e., the photonic band gap [shown in Fig. 1(b)], while the nonzero transmission coefficient corresponds to the allowed "band" of photons. It is well known that in a random system, photons cannot propagate in a wide frequency region [as shown in Figs. 1(c) and 1(d)]. By comparing with Figs. 1(b) and 1(d), it is obvious that a different photonic band appears in the dispersion relationship in the RD case. Actually, in an infinite RD case, this band will be reduced to a single mode satisfying Eq. (10) in the case of $n=2$, i.e., $\omega_{RD}=\pi c/2a$. (Here c is the light velocity in vacuum.) This feature indicates that the localization-delocalization transition of photons takes place at the specific frequency in a RD system and the resonant mode obeys Eq. (10) (here $n=2$).

In order to demonstrate localization-delocalization transition of photons in a RD multilayer, the spatial distribution of an electric field has been calculated. Figure 2 shows the electric field distributions in the RD multilayer of SiO_2/TiO_2 at some frequency regions. It turns out that when photon possesses the resonant frequency $\omega_{RD}=\pi c/2a$, the electric field amplitude is extendedly distributed in the RD multilayer and the electromagnetic wave propagates through the whole RD system without decay [as shown in Figs. 2(a) and 2(b)]. Figure 2 also provides critical amplitude distributions [as shown in Figs. 2(c) and 2(d)] and localized amplitude distributions [as shown in Figs. 2(e) and 2(f)] when the frequency of the photon deviates from the resonant mode. In those cases, the electromagnetic wave cannot propagate in the whole system [as indicated in Figs. 2(c)–2(f)]. Therefore, at the resonant frequency, the localization-delocalization transition of photons occurs, indeed, in the RD system.

IV. RANDOM *n*-mer CASE

The results of the RD structure can be generalized to the random RN model described by Eq. (6). Figure 3 presents photonic transmission and the density of states of photons in several RN SiO_2/TiO_2 multilayers. According to Eqs. (10)–(12), delocalization of photons will happen at resonant frequencies satisfying Eq. (10), i.e., $\omega_R=(l/n)(\pi c/a)$, where $l=1,2,\ldots,n-1$. Therefore, $n-1$ resonant peaks appear in the transmission spectrum of the RN dielectric structure [as shown in Figs. 3(a)–3(e)]. For instance, there are one transmission peak in the spectra of a random-dimer structure, two peaks in a random-trimer chain, three peaks in a random 4-mer chain, and four peaks in a random 5-mer chain, respectively. Adjacent to the resonant frequency, a new channel is opened for photonic transmission. Therefore, the density of states of photons has an enhancement around each resonant frequency [as shown in Figs. 3(f)–3(j)]. Hence the density of states of photons is enhanced around each corresponding resonant frequency. As a result, the density of states increases step by step as the frequency increases in the RN dielectric system.

Delocalization of photons in the RN system can also be characterized by a zero-Lyapunov exponent at the resonant mode. It is known that one important parameter to characterize the physical nature of random matrices is the Lyapunov coefficient.[17] In a 1D dielectric system, the Lyapunov coefficient can be expressed as

$$\Gamma = \frac{1}{N}\ln(m_{11}^2 + m_{12}^2 + m_{21}^2 + m_{22}^2), \tag{13}$$

where m_{ij} $(i,j=1,2)$ is the element of the global matrix $M(N,\delta_i)$. According to the Furstenberg theorem,[18] the Lyapunov coefficient exists and converges to its mean value for a sufficiently large system. In fact, in a dielectric system, the Lyapunov coefficient is inverse to the localization length of photons. Once the length of the sample is sufficiently long, the zero-Lyapunov coefficient corresponds to delocalized states with infinite localized length. Therefore, based on the Lyapunov coefficient, we can obtain the overall behavior of the photons; i.e., we can know whether they are localized or delocalized at specific frequencies in the system. Figure 4 shows Lyapunov coefficients as a function of photonic frequency in several RN structures. It can be seen that around

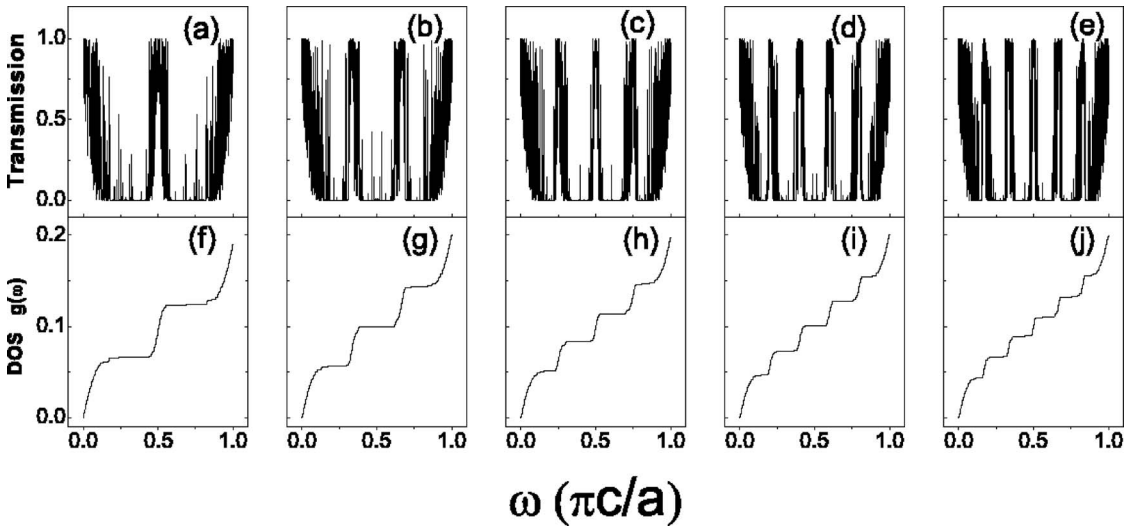

FIG. 3. The transmission coefficient and the density of states $g(\omega)$ as a function of the frequency in several RN multilayers. (a) and (f), a random-dimer multilayer with $N=365$; (b) and (g), a random-trimer multilayer with $N=480$; (c) and (h), a random-tetramer multilayer with $N=595$; (d) and (i), a random 5-mer multilayer with $N=710$; and (e) and (j), a random 6-mer multilayer with $N=825$. Other parameters are the same as in Fig. 1.

resonant frequencies in each structure, the Lyapunov coefficient approaches zero even though fluctuation exists [as shown in Figs. 4(a)–4(e)]. Actually, fluctuation can be eliminated when the number of layers in the structure increases. Due to the fact that the zero-Lyapunov coefficient appears at the resonant frequencies, the localized length of photons is infinite at these frequencies. At these modes, photons cannot "feel" defects in the structure and can transport through the multilayer without decay. Therefore, delocalization of photons occurs at each resonant mode in the RN system, and the total number of resonant modes in the system is $n-1$. Each delocalization of photons opens a channel for photonic transport; finally, the density of states of photons increases step by step.

V. EXPERIMENTAL RESULTS

To demonstrate the above theoretical analysis, we have carried out the experiments on the RN dielectric multilayer films. Silicon dioxide (SiO_2) and titanium dioxide (TiO_2) were chosen as dielectric materials A and B, respectively. By electron-gun evaporation method, several RN multilayer films of SiO_2/TiO_2 were fabricated on the glass substrate. Before evaporation, the pressure of the chamber was lower than 2×10^{-5} Torr. Then, the films were formed in an oxygen atmosphere: the pressure was 0.8×10^{-4} Torr for SiO_2 deposition and 2×10^{-4} Torr for TiO_2 deposition. The thicknesses of these two materials were chosen to satisfy $n_Ad_A=n_Bd_B$. The central wavelength was set around $\lambda_0=700$ nm. Therefore, $d_A=(700\text{ nm})/4n_A\approx119.0$ nm, and $d_B=(700\text{ nm})/4n_B\approx76.1$ nm. During the deposition, the thickness of the film was controlled by quartz crystal monitoring at a frequency of 5.0 MHz, and also the quarter-wave optical thickness was optically monitored. As an example, the structure of the RD SiO_2/TiO_2 film was characterized by a field emission scanning electron microscope (LEO 1530VP). In

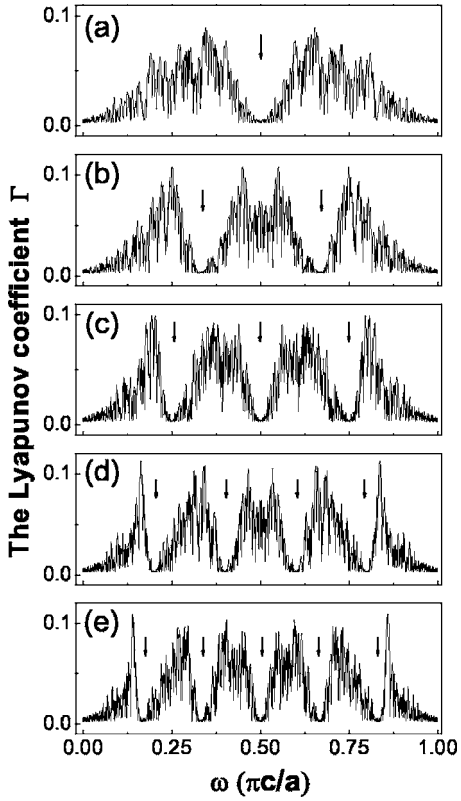

FIG. 4. The Lyapunov coefficient Γ as a function of the frequency in several RN multilayers. (a) A random-dimer multilayer with $N=365$, where $\omega_{RD}=(1/2)(\pi c/a)$; (b) a random-trimer multilayer with $N=480$, where $\omega_R=(1/3)(\pi c/a)$, $(2/3)(\pi c/a)$, respectively; (c) a random-tetramer multilayer with $N=595$, where $\omega_R=(1/4)(\pi c/a)$, $(1/2)(\pi c/a)$, $(3/4)(\pi c/a)$, respectively; (d) a random 5-mer multilayer with $N=710$, where $\omega_R=(1/5)(\pi c/a)$, $(2/5)(\pi c/a)$, $(3/5)(\pi c/a)$, $(4/5)(\pi c/a)$, respectively; and (e) a random 6-mer multilayer with $N=825$, where $\omega_R=(1/6)(\pi c/a)$, $(1/3)(\pi c/a)$, $(1/2)(\pi c/a)$, $(2/3)(\pi c/a)$, $(5/6)(\pi c/a)$, respectively. Other parameters are the same as in Fig. 1.

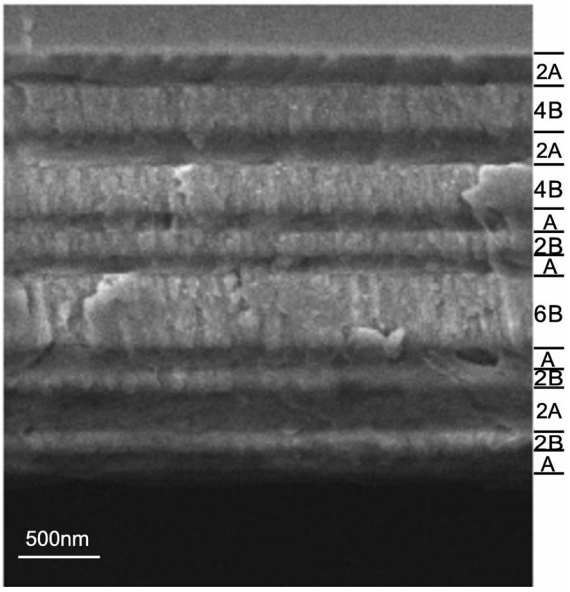

FIG. 5. Cross-sectional SEM image of the RD SiO_2/TiO_2 multilayer film with $N=30$. The RD sequence is marked, where dielectric materials A and B are SiO_2 and TiO_2, respectively. Note that the cross section of the sample has not been polished, and in order to increase the conductivity, the sample is covered by a gold film with a thickness of 5 nm or so.

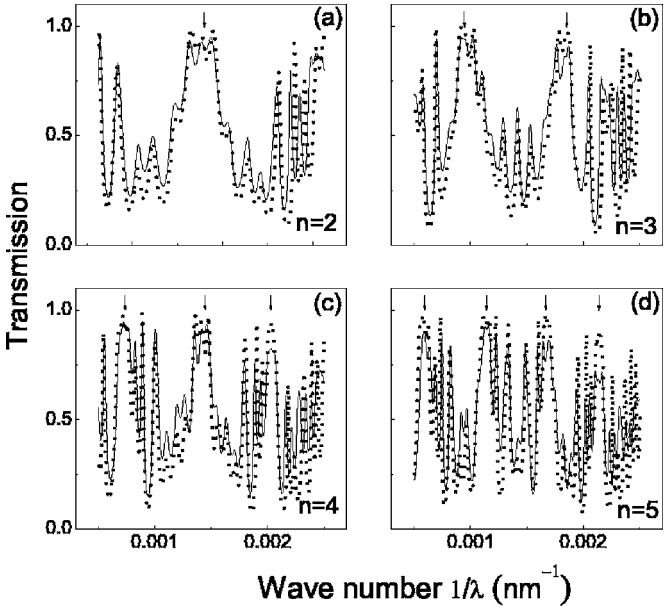

FIG. 6. The measured and calculated transmission coefficient T as a function of the wave number λ^{-1} in the RN multilayer films of SiO_2/TiO_2. (a) A random-dimer multilayer with $N=30$, and (b) a random-trimer multilayer with $N=40$, (c) a random-tetramer multilayer with $N=50$, and (d) a random 5-mer multilayer with $N=60$. Note that in each figure, the solid curve is for the measured spectrum, while the dashed curve is for the calculated one. Here absorption of dielectric materials has been included.

order to increase the conductivity, the sample is covered by a gold film with a thickness of 5 nm or so. Figure 5 shows a cross-sectional scanning electron microscope (SEM) image of the RD multilayer of SiO_2/TiO_2. The layered structure and the RD sequence are clearly revealed as marked in Fig. 5.

The optical transmission spectra of the multilayer films have been measured by PerkinElmer Lambda 900 spectrophotometer in the range of wavelength from 400 to 2000 nm. Figure 6 shows the measured and calculated transmission spectra of several RN SiO_2/TiO_2 multilayer films for $n=2$, 3, 4, and 5. It is demonstrated that $n-1$ resonant peaks indeed exist in the RN multilayers of SiO_2/TiO_2 [as marked by the arrows in Figs. 6(a)–6(d)]. Due to the fact that the number of dielectric layers is very limited in each film, each resonant peak becomes wide instead of a δ-functional peak at $\omega_R=(l/n)(\pi c/a)$, where $l=1,2,\ldots,n-1$. In other words, each resonant peak is broaden to a resonant band. Therefore, around the resonant frequency ω_R, the localization-delocalization transition of a photon has occurred as predicted in the RN dielectric system.

VI. SUMMARY

To summarize, we have investigated the photonic transmission, the dispersion relation, and the density of states of 1D random n-mer $(n=2,3,4,\ldots)$ dielectric systems. The localization-delocalization transitions of photons have been demonstrated in this correlated disorder system. Multiple resonant transmissions are observed, which agrees with the analytical expectation. At each resonant mode, zero-Lyapunov exponent and undecayed field distribution have been found through the whole system. Meanwhile, channels are opened for photon transport. As a result, the density of states is enhanced significantly at each resonant mode. The localization-delocalization transition of photon has been demonstrated experimentally by the observations on the SiO_2/TiO_2 multilayer films in visible and near-infrared regions of light. The photon behavior presented here provides a possible way to manipulate the photons in the photonic band gap and may have applications in designing filters and waveguide of electromagnetic waves.

ACKNOWLEDGMENTS

This work was supported by grants from the National Natural Science Foundation of China (Grant Nos. 10625417, 50672035, and 90601001), the State Key Program for Basic Research from the Ministry of Science and Technology of China (Grant Nos. 2004CB619005 and 2006CB921804), and partly by the Ministry of Education of China (Grant No. NCET-05-0440).

*Author to whom correspondence should be addressed. Electronic address: rwpeng@nju.edu.cn

[1] P. W. Anderson, Phys. Rev. **109**, 1492 (1958).
[2] S. He and J. D. Maynard, Phys. Rev. Lett. **57**, 3171 (1986); D. T. Smith, C. P. Lorenson, R. B. Hallock, K. R. McCall, and R. A. Guyer, *ibid.* **61**, 1286 (1988).
[3] L. Tsang and A. Ishimaru, J. Opt. Soc. Am. A **2**, 2187 (1985); M. P. van Albada, M. B. van der Mark, and A. Lagendijk, Phys. Rev. Lett. **58**, 361 (1987); P. E. Wolf and G. Maret, *ibid.* **55**, 2696 (1985).
[4] S. John, Phys. Rev. Lett. **58**, 2486 (1987); Phys. Today **44**(5), 32 (1991).
[5] K. Machida and M. Fujita, Phys. Rev. B **34**, 7367 (1986); P. Hu and C. S. Ting, *ibid.* **34**, 8331 (1986); Y. Liu and R. Riklund, *ibid.* **35**, 6034 (1987).
[6] M. Kohmoto and J. R. Banavar, Phys. Rev. B **34**, 563 (1986).
[7] R. W. Peng, M. Wang, A. Hu, S. S. Jiang, G. J. Jin, and D. Feng, Phys. Rev. B **57**, 1544 (1998); R. W. Peng, Y. M. Liu, X. Q. Huang, F. Qiu, Mu Wang, A. Hu, S. S. Jiang, D. Feng, L. Z. Ouyang, and J. Zou, *ibid.* **69**, 165109 (2004).
[8] S. Aubry and G. André, Ann. Isr. Phys. Soc. **3**, 133 (1980).
[9] M. Dulea, M. Johansson, and R. Riklund, Phys. Rev. B **45**, 105 (1992).
[10] E. Yablonovitch, Phys. Rev. Lett. **58**, 2059 (1987); E. Yablonovitch, T. J. Gmitter, and R. Bhat, *ibid.* **61**, 2546 (1988); E. Yablonovitch and T. J. Gmitter, *ibid.* **63**, 1950 (1989).
[11] J. D. Joannopoulos, P. R. Villeneuve, and S. Fan, Nature (London) **386**, 143 (1997).
[12] D. H. Dunlap, H. L. Wu, and P. W. Phillips, Phys. Rev. Lett. **65**, 88 (1990).
[13] P. Phillips, Annu. Rev. Phys. Chem. **44**, 115 (1993); D. Giri, P. K. Datta, and K. Kundu, Phys. Rev. B **48**, 14113 (1993); R. Farchioni and G. Grosso, *ibid.* **56**, 1170 (1997); S. N. Evangelou and E. N. Economou, J. Phys. A **26**, 2803 (1993); Y. M. Liu, R. W. Peng, X. Q. Huang, Mu Wang, A. Hu, and S. S. Jiang, Phys. Rev. B **67**, 205209 (2003).
[14] V. Bellani, E. Diez, R. Hey, L. Toni, L. Tarricone, G. B. Parravicini, F. Domínguez-Adame, and R. Gómez-Alcalá, Phys. Rev. Lett. **82**, 2159 (1999).
[15] S. Sil, S. N. Karmakar, R. K. Moitra, and A. Chakrabarti, Phys. Rev. B **48**, 4192 (1993); A. Chakrabarti, S. N. Karmakar, and R. K. Moitra, Phys. Rev. Lett. **74**, 1403 (1995).
[16] E. Maciá, Phys. Rev. B **73**, 184303 (2006).
[17] E. Maciá, Phys. Rev. B **61**, 6645 (2000); L. S. Cao, R. W. Peng, R. L. Zhang, X. F. Zhang, Mu Wang, X. Q. Huang, A. Hu, and S. S. Jiang, Phys. Rev. B **72**, 214301 (2005).
[18] K. Ishii, Suppl. Prog. Theor. Phys. **53**, 77 (1973), and references therein; P. D. Kirkman and J. B. Pendry, J. Phys.: Condens. Matter **17**, 4327 (1992).